JOURNAL OF MATERIALS SCIENCE 17 (1982) 1649–1655

Fracture-induced photon emission of aluminium oxide and its application to fracture mechanical investigations

A. KRELL
Akademie der Wissenschaften der DDR, Zentralinstitut für Festkörperphysik und Werkstofforschung, 8027 Dresden, DDR

Mechanically-stimulated luminescence is generated during sub-critical crack growth prior to macroscopic bending fracture of sintered alumina, fusion-cast Al_2O_3, sapphire, and ruby. At similar toughness, K_{Ic}, the measured intensity increases with the hardness of the tested specimens, it does not depend on the macroscopic fracture strength.

1. Introduction

Tribo-physical effects have been investigated by many authors for a wide range of substances [1–7]. Commonly, a continuous emission of photons or electrons is measured during a longer time interval of constant mechanical treatment of the solid body, for example, by grinding, scratching, drilling, hard-particle blasting techniques or under compression. In most of such experiments the main question concerns the nature of the emission process. As a consequence of the techniques used irregular fracture geometries arise. It is the aim of the present paper to demonstrate that mechanically stimulated luminescence can supply useful information concerning the mechanics of crack propagation in a brittle solid if a more defined crack geometry is provided. To distinguish this technique from abrasive activation methods the term fracture-induced photon emission (FIPE) is preferred to the traditional designation as triboluminescence (TL or TBL).

2. Experimental procedure

2.1. Apparatus

A bending force is horizontally given, to a 3-point-bending appliance acting on the specimen, the surface under tension of which is directed to the front window of a photomultiplier.* The distance between sample and photomultiplier is 11 mm, the span length is chosen as 14 mm and the cross-head speed selected is about 3 mm min^{-1}.

To prevent a recording of emission due to friction between specimen and the bearing steel bolts of the bending device, a metal screen covered with black rubber and having a slit window of 7 mm width is placed between the fracturing surface of the sample and the photomultiplier. The influence of this screen was tested using alumina specimens completely wrapped in paper several millimetres thick to eliminate friction and with only a small surface area at the very locus of fracture being exposed to the photomultiplier. Such specimens gave similar results without the screen as uncovered samples did with the screen. Obviously, all of the luminescence contribution from friction is taken away by the screen whereas, on the other hand, there is no loss of emission emerging from fraction of the specimen.

Gas discharge on electrified fracture surfaces, as described in [8, 9], is prevented by maintaining a vacuum of about 10^{-2} Pa during fracture tests.

The one quantity recorded is the sum of emission counts for the whole fracture process; in some experiments the fracture strength is measured simultaneously, with an accuracy of about 3%. The number of dark counts was no more than one per fracture test.

Since, for the chosen amplification conditions, the pulse duration is about 0.5 μsec (measured

*Photomultiplier model M12 FVC 51, manufactured by Werk für Fernsehelektronik, Berlin, DDR.

0022–2461/82/061649–07$03.34/0

with an oscillograph), the equipment is unable to register more than two counts per microsecond.

2.2. Specimen materials

Alumina bars were fabricated by granulating and pressing 0.3 μm powder with a lubricant and sintering it to a density of 3.89 to 3.94 g cm^{-3} and average grain sizes smaller than 10 μm. In addition to the usual structures a series of specimens with a not fully developed (under-fired) bi-disperse grain-size distribution has been investigated. Structural data and mechanical properties are presented in Section 4.2 and discussed in detail elsewhere [10].

To test the influence of a special dopant on the specific emission per microscopic crack area, flat specimens were cut from Verneuil boules of sapphire and ruby* (0.5 and 3.4 wt% Cr). Samples from different sapphire boules gave emission results that could differ by a factor of between 2 and 3. All of the plates were of such an orientation that a rough fracture surface macroscopically near (0 0 0 1) was produced; microscopic fracture were preferably along ($\bar{1}$ 0 1 2) and (1 0 $\bar{1}$ 4). This orientation is suitable for inducing comparable crack structures near the stressed specimen surface: if fracture occurs along one crystallographically-defined easily-spalling lattice plane a dopant-dependent toughness must be assumed to alter the cracking behaviour significantly, but, similarly, if rough fracture surfaces are generated, this influence is supposed to be removed. In addition to this, an equivalent density of flaws was generated by notching the 4 mm thick samples to a depth of about 0.5 mm with a diamond wheel of 40 to 60 μm grain size.

Fusion cast corundum† without Cr (white in colour) and with about 1.4 wt% Cr (dark red in colour) had a grain size of 300 to 900 μm and a porosity of 30 to 60%.

3. Experimental results

Experiments with dense alumina specimens of 6.5 mm x 6.5 mm cross-section yielded at the used amplification conditions 10 to 55 000 counts, depending on the grain structure. The emission occurred in the moment of macroscopic fracture, independent of the actual fracture stress. Therefore, and since luminescence due to friction between sample and bending appliance can be ruled out, the registered emission must have been generated during the propagation of the main crack cutting through the specimen.

The final velocity of catastrophic crack propagation is about 10^3 m sec^{-1}. When the stress intensity reaches its critical value, K_{Ic}, the crack shows such an acceleration [11] that the specimen breaks within some microseconds only. Therefore, due to the recording capacity, only a few counts shall be registered during unstable fracture. The high yield of observed luminescence, however, indicates a minimum process duration of 5 μsec to 27 msec, which agrees fairly well with oscillographic measurements. Consequently it must be some process of stable (i.e., slower) crack growth immediately before instability that activates the luminescence. Since macroscopic fracture of the alumina samples is initiated by the worst surface flaw, the stress concentration at the tip of this sub-critically growing defect within the stressed surface is supposed to activate the emission. To compare different samples, obviously, the number of counts recorded during stable crack growth must not be related to the nearly "dark" area of unstable fracture (specimen height x width) but to the crack length across the specimen width as this is "visible" to the photomultiplier. Generally, if only a single main crack develops from one fracture initiating flaw and if no macroscopic branching occurs, this crack length finally equals the width of the stress specimen surface.

Tests with simultaneous recording of FIPE intensity, I, and fracture strength, σ_f, revealed no clear dependence for aluminas of different grain structure (see Fig. 1a). To find the reason for this, precision Vickers hardness measurements were made using a load of 98.1 N maintained for 15 sec, as recommended by the results of another investigation [12]. Ranking the intensity values of the same specimens as in Fig. 1a, according to their hardness, H_v, gives a clear dependence of the form

$$I \propto \exp H_v \qquad (1)$$

for both structures (see Fig. 1b). Using an indentation technique [13] all the specimens of the series were shown to have a toughness within ± 10% of the average given in Fig. 1.

Fig. 2 compares emission results for other structures differing in their median grain sizes, $\bar{D}$. Specimens with $\bar{D}$ of 8 to 10 μm (not included in

*From Chemiekombinat Bitterfeld, DDR.
†From Elektroschmelze Zschornewitz, DDR.

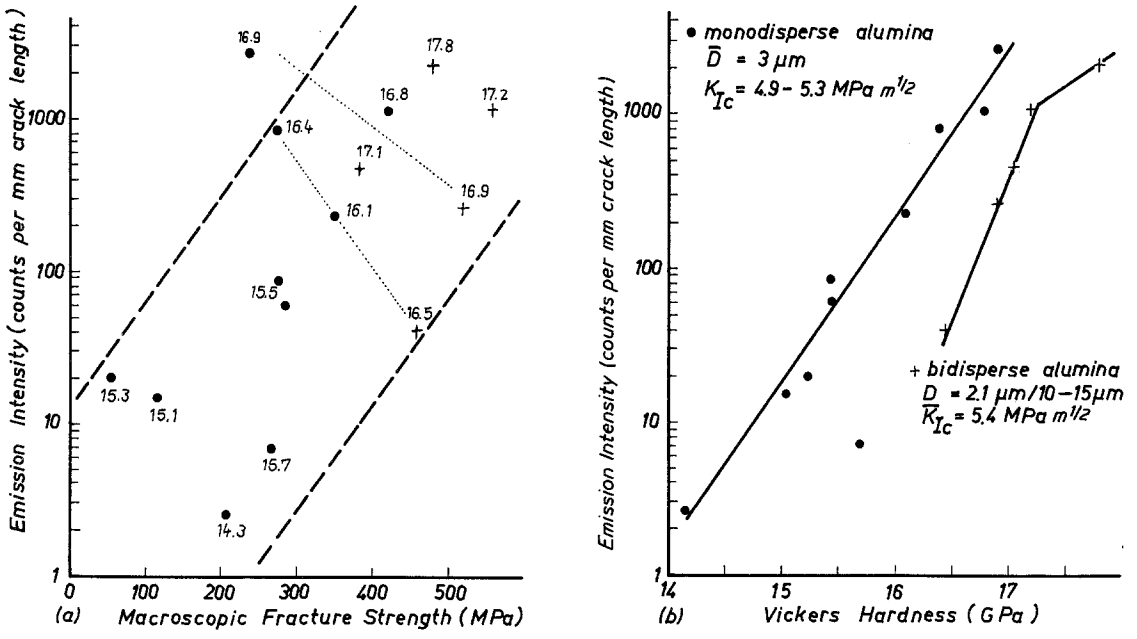

Figure 1 Dependence of FIPE intensity, I, on (a) fracture strength, σ_f, and (b) Vickers hardness, H_v, for dense alumina. In Fig. 1a numbers at data points give H_v(GPa).

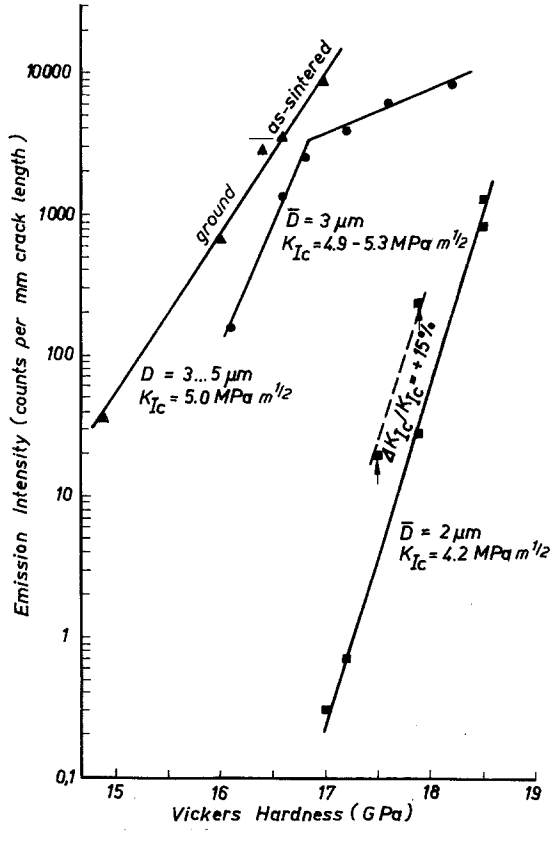

Figure 2 Fracture luminescence of different aluminas with homogeneous grain-size distribution.

Fig. 2) followed the same dependence as in Equation 1. At a given hardness a higher intensity is observed for coarser structures. For the finest grain structure, samples with enhanced fracture toughness, K_{Ic}, gave intensified luminescence.

No change of the emission behaviour was seen to occur when ground (10 to 15 μm diamond wheel) surfaces are investigated instead of as-sintered ones. In contrast to the samples for which the FIPE results are represented in Fig. 2, average H_v and K_{Ic} values are not affected by the grinding operation for this kind of structure; the strength is increased by 43%, indicating a change of the flaw structure.

Fig. 3 shows the results for sapphire and ruby, average over three to four measurements of I, against Cr-concentration. With increasing Cr contents a modest but continuous intensification of luminescence is observed.

A more rigorous influence of Cr-doping is found for fusion-cast corundum: due to the Cr additions unnotched specimens revealed an increase in intensity, I, of a factor of about 40 (see Table I). In order to check whether in this special case the observed increase could have been caused by retarted crack propagation resulting in an increase of emission events being resolved by the electronics, an experiment was conducted at slow loading to

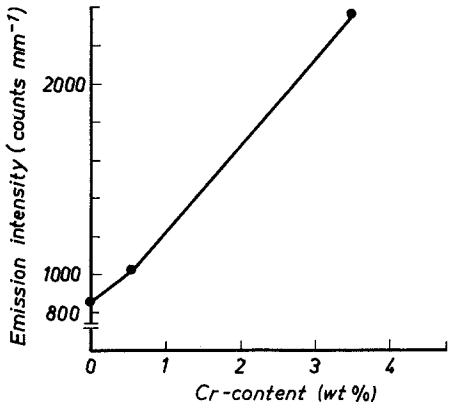

Figure 3 Influence of chromium additions on FIPE intensity of single-crystal Al_2O_3.

promote this tendency for a slower fracture progress. The observed further increase in emission intensity could be generated by more extensive microcracking on the specimen surface or by a general slowing of the macroscopic fracture process, therefore an attempt was made to study emission from a deeply-notched (to half the specimen depth) sample, in order to try to eliminate emission from the specimen surface. (The specimens used were thicker, in such a way that the remaining cross-section of the notched samples to be broken equalled the thickness of the unnotched samples used elsewhere in this work.)

In these experiments the observed intensity was related to the fractured cross-sectional area. To prevent a ready transition to stable cracking, as a consequence of the introduced notch, the samples, as usual, were loaded rapidly. Comparing, at one loading speed, unnotched and notched Cr-containing bars (see Table I), the relatively high-intensity values for the notched bars point to the possibility that a great part (about 40%) of the registered intensity emerges not from the specimen surface, but from a large part of the fracture area itself as it is generated in the course of crack propagation. A similar result arose on a macroscopically unnotched specimen with a natural sharp notch supplied by preceding stable crack propagation. Altogether Table I indicates an increasing luminescence with growing tendency to slower cracking due to Cr-additions and slower loading for fusion-cast corundum.

4. Discussion

4.1. Mechanical activation of luminescence

Luminescence is generated by the mechanical activation of centres of electronic disorder which are assumed to be homogeneously distributed with a spacing small compared with the dimensions of crack propagation. The finest-grained structure included in the FIPE investigations (see Fig. 2) had been sintered in air, whereas all the other sample series were fabricated in dry hydrogen. Sintering in air is assumed to be the reason for the low emission intensities reported by several authors [14, 15], since F^- and F^+-centres (anionic vacancies containing one or two electrons) are generated more easily during high-temperature treatment in H_2 than in air. Therefore, the lower defect concentrations of the air-sintered samples must result in lower emission intensities on activation.

Results on alkali halides and MgO [9, 16] lead to the conclusion that mechanoluminescence can only be activated by fracture-surface generation or if high microplastic strain is initiated by localized stresses scaling the yield stress. With regard to the high yield stress of Al_2O_3, which at room tem-

TABLE I Luminescence of fusion cast corundum, dependent on Cr-additions. Results are related to 100% dense material

Sample	Cross-head velocity (mm min^{-1})	FIPE intensity, I	
		Counts per mm crack length	Counts per mm^2 fracture surface
White corundum	3	35	(8)
Corundum + 1.4 wt% Cr*	3	1280	480
	< 3	2040	860
Corundum + 1.4 wt% Cr†	3	380	215
Single-crystal sapphire with no Cr addition	3	365	–
Single-crystal ruby + 2 wt% Cr	3	1700	–

*Unnotched
†Notched

perature is between 4.5 and 7.5 GPa, depending on the structure [17], it is clear that in bending experiments such an amount of microstrain is possible only at the highly-stressed tip of some propagating crack. In the preceding section it had been shown that processes at the tip of the one fracture-initiating main crack are largely responsible for the FIPE emission. Another argument for the localized character of the emission processes is the observed insensibility of the intensity to surface grinding (see Fig. 2). If luminescence is generated from cracks all over the specimen surface, at increasing load, independent of the stress concentration of the main crack, then, in contrast to the experimental finding, the measured intensity should strongly reflect the altered density of cracks produced due to the changed flaw structure after grinding. Assuming, however, that luminescence is mainly associated with processes at the tip of only one fracture-initiating main crack, the experimental result is readily understood. Of course, the recorded emission need not be solely generated by the subcritical propagation of a single main crack-front, but may emerge also from microcracking within the stress concentration zone at this crack tip.

4.2. Luminescence from fracture of sintered alumina

There exists no clear correspondence between fracture strength and luminescence (see Fig. 1a), since the mechanical activation only depends on the local stress level at the crack tip and not on the macroscopic strength which, at one K_{Ic} value, must show a scatter due to the differences in the fracture-initiating flaw sizes of the specimens.

Ranking the same FIPE results according to their respective sample hardness reveals a relation of the form of Equation 1. The increase of intensity with hardness can be understood considering the physical structure of the Vickers hardness. Fröhlich *et al.* [18] demonstrated that the conventionally measured hardness, H_v, comprises contributions from several processes, and several types of hardness numbers can be separated experimentally:

(a) $H_v(P_2)$, the "crack-free" inherent hardness of the lattice itself (for sapphire $H_v(P_2)$ has a value of 10 GPa independent of indenter load [12]);

(b) $H_v(P)$, the conventional hardness but measured under load (additionally comprising surface effects like cracking and friction) decreases with increasing load, P (for sapphire $H_v(P)$ is about 11 GPa at $P = 98.1$ N [12]); and

(c) H_v, which exceeds $H_v(P)$ due to elastic relaxation since it is measured after unloading (for sapphire, H_v is 15 GPa after $P = 98.1$ N for 15 sec [12]).

Therefore, existing within one kind of structure, minor variations in the median grain size ($\Delta\bar{D}/\bar{D} \approx 5\%$) and the associated change in the microcracking behaviour ($\Delta\rho/\rho \approx 2$ to 20%, where ρ is the microcrack density on the fracture surface [10]) can result in variations of $H_v(P)$ and H_v dependent on the real specimen structure. If at very high ρ microcracks around the indentation link up and large-area cracking causes low values for H_v, additional variations of the elastic relaxation can generate a further scatter in hardness. On 3-point-bending the stress concentration at the tip of the main crack plays the role of the localized indenter stress field. During fracture of specimens with higher apparent hardness due to the higher contributions from surface effects, this stress concentration can produce a higher ρ value. Therefore, an increased luminescence from microcracking will arise for specimens with enhanced H_v. Within one series this is possible at unchanged K_{Ic} since over a wide range of ρ there is no remarkable influence of ρ on K_{Ic}, as it was shown by theory [19] and experiment [10]. If, however, samples with different K_{Ic} are to be compared, I can increase, decrease or remain unchanged due to the actual co-operation of microscopic relaxation effects at the crack tip and resulting differences between macroscopic and microscopic K_{Ic} levels, as described by the microcrack model [19, 20] and discussed elsewhere in more detail [21]. Consequently, without additional work, no conclusions concerning the relevant K_{Ic} can be drawn from luminescence results. Comparing samples sintered at the same atmosphere and having a given hardness, generally a higher intensity is observed for the specimens with the larger grain size (see the upper two curves in Fig. 2). This is due to the above described susceptibility of coarser structures to large-area cracking, resulting in a low average hardness.

Comparing, in Fig. 1a, intensity values of specimens with nearly the same hardness, it can be seen that there is no general increase of I with the fracture strength. Actually, the trend of intensified emission for high-strength samples is caused by the increased hardness of these structures, as demonstrated by Fig. 1. This accentuates the primary

TABLE II Structure and properties of homogeneous and bi-disperse aluminas. $\rho = 1.0$ for the under-fired bi-disperse samples is estimated from $\rho = 1.16$, as measured for the fully developed structure with $K_{Ic} = 7$ to 8 MPa $m^{1/2}$

Sample	Grain-size structure	ρ	$\bar{\sigma}_f$ (MPa)	$\overline{K_{Ic}}$ (MPa $m^{1/2}$)	I (for H_v constant) (Relative units)
Homogeneous	$\bar{D} \approx 3.0\,\mu m$	1.4	290 ± 26	4.7–5.3	1.00
Bi-disperse (under-fired)	$\bar{D}_1 = 2.1\,\mu m$; $\bar{D}_2 = 10$ to $15\,\mu m$ (75 vol% D_1 + 25 vol% D_2)	1.0	400 ± 45	5.4	0.06–0.27

character of the I–H_v dependence. The bi-disperse samples emitted a lower luminescence than the homogeneous structure with similar average grain size (see Fig. 1b). Fig. 1a demonstrates the better strength characteristic of the bi-disperse structure, which was slightly under-fired to get a narrow strength distribution with only a modest increase of K_{Ic}. Table II compares the data for the two structures from Fig. 1; details concerning the measurement conditions for σ_f, K_{Ic} and the microcrack density, ρ, are described elsewhere [10]. As discussed previously [10], the strengthening effect can be attributed to crack-front pinning by "hard" inclusions (that is, the larger grains) [22, 23] or be attributable to microcracking [19, 20].

The second theory distinguishes between additional energy dissipation by residual stress-induced microcracking within a relatively large dissipation zone and toughness-diminishing effects of microcracks in a narrow process zone at the very tip of the main crack. Therefore, a screening mechanism around this tip can influence the amount of subcritical crack propagation (and thus the amount of FIPE emission), changing the ratio of the onset of subcritical growth and final instability. This, together with the observed lower microcrack density of the bi-disperse structure (compared with the homogeneous alumina of about equal median grain size), can explain the lower FIPE intensity of the first structure.

Using the pinning model, the effect is difficult to explain. There is no possibility of local stress relaxation, and therefore the decrease of I can be related to the decrease of ρ only as given in Table II. In this way a decrease to about 100/140 = 71% of the intensity observed for homogeneous samples had to be expected for the bi-disperse structure, which disagrees with the experimental result of only 6 to 27% (see Table II). Consequently, the luminescence behaviour of the bi-disperse series is considered as an evidence for microcracking as the main mechanism, which causes the increase in σ_f and K_{Ic} of this material.

The increase of K_{Ic} due to microcracking occurs rather suddenly at some crack density [10]. A similar influence on hardness might be the reason for the strong rise of H_v observed as a changing slope of several curves when I exceeds a critical value (see Fig. 1b and 2).

4.3. Sapphire and ruby

As a consequence of the preparation procedure and the almost equal mirror constants (i.e., K_{Ic}) for $(\bar{1}\,0\,1\,2)$-fracture than can be estimated from fractographic examinations of sapphire and ruby, reported by Abdel-Latif *et al.* [24], the result of Fig. 3 can be attributed to different specific emission during similar fracture processes.

The effect is thought to be due to the activation of an increasing number of centres of electronic disorder, although constant electrical conductivity up to 0.7 wt% Cr points to an unchanged state of valence [25]. An influence of Cr^{3+} on the luminescence, without affecting the conductivity, seems to be possible, taking into consideration the large width of 15 to 30 eV found for the two- or even three-fold split valence band and the wide energy-gap of 10 eV between the valence and conduction bands [26]. Indeed, it was found that in Verneuil crystals, 0.001 to 0.030 wt% Cr contents are sufficient to generate intensive colouration [27] and thermoluminescence from the recombination of holes with F-centres [15]. Such centres can be introduced by irridiation [28] or by thermal treatment [14].

4.4. Fusion-cast corundum

In the case of Cr-containing material, the experiments indicate contributions to the registered intensity coming from a large part of the fracture surface itself. Therefore, with regard to the counting capacity of 2 counts μsec^{-1} it is supposed that the Cr-dopant leads to a decrease of the final fracture velocity, which is about 10^3 m sec^{-1} for usual instability. This hypothesis was supported by oscillographic tests pointing to an average velocity of only 6×10^{-3} m sec^{-1} for notched and rapidly-loaded specimens, which is not far away from the

velocity where the crack becomes unstable. Also, even unnotched Cr-containing samples sometimes fractured in either an unstable or stable manner if they were slowly loaded. This stable fracture is accompanied by a very high yield of emission. Without Cr, stable fracture has never been observed, not even on slowly loading notched bars.

Cr-containing fusion-cast specimens fracture preferentially in an intergranular manner. Comparing with the results found on single crystals, it seems that chromium affects the mechanical properties of grain boundaries of the fusion-cast material much more than those of the crystal lattice. Since such an effect can result from the specific structure of boundaries at one dopant concentration throughout the lattice, it does not contradict the observed lack of Cr-enrichment at boundaries in dense alumina [29].

5. Conclusions

Using suitable conditions, sufficient luminescence from subcritical crack growth can be recorded at usual bending tests for fracture mechanical investigations of Al_2O_3. Although sometimes an increase in toughness, K_{Ic}, is accompanied by a higher emission intensity, I, due to changes of the basic micromechanisms, this need not be true in every case. Therefore, no general correlation between I and K_{Ic} or fracture strength, σ_f, can be observed. Concerning the Vickers hardness, H_v, at constant K_{Ic}, a relation of the form $I \propto \exp H_v$ has been found. Generally, for aluminas with $\bar{D} < 10\,\mu m$ at a given hardness, I, increases with growing grain size. The FIPE behaviour of a bi-disperse structure with enhanced mechanical properties indicates an active microcrack mechanism causing the increase in strength and toughness.

Chromium only modestly intensifies the specific emission of Al_2O_3 single crystals. It decreases the velocity of catastrophic fracture of fusion-cast corundum by almost six orders of magnitude. The effect is proposed to reflect a stronger influence of Cr on the mechanical properties of grain boundaries than on those of the crystal lattice.

Acknowledgements

The author wishes to thank Professor D. Schulze for stimulating the luminescence investigations presented here and for valuable supporting advices. He acknowledges the co-operation with Dr A. S. Maslov and Dipl.-Ing R. Gärtner who developed the mechanical and electric construction of the FIPE apparatus. The author is obliged to Dr E. Linke and co-workers at the Central Institute for Physical Chemistry of the Academy of Science of the GDR in Berlin for critical discussion of first results.

References

1. P. A. THIESSEN, K. MEYER and G. HENNICKE, Grundlagen der Tribochemie, Akademie-Verlag, Berlin, 1967.
2. K. HOFFMANN and E. LINKE, *Kristall und Technik* **12** (1977) 495.
3. *Idem, ibid.* **11** (1976) 835.
4. L. SODOMKA, *Phys. Stat. Sol. (a)* 7 (1971) K65.
5. G. BATHOW, *Naturwiss.* **45** (1958) 381.
6. B. P. CHANDRA, P. R. TUTKANE, R. D. VERMA and M. ELYAS, *Kirstall und Technik* **13** (1978) 71.
7. F. FRÖHLICH and P. SEIFERT, *Crystal. Lat. Def.* **2** (1971) 239.
8. M. I. KORNFELD, *J. Phys. D* **11** (1978) 1295.
9. L. M. BELYAEV and Yu. N. MARTYSHEV, *Phys. Stat. Sol.* **34** (1969) 57.
10. A. KRELL, *Phys. Stat. Sol. (a)* **63** (1981) 183.
11. J. CONGLETON and N. J. PETCH, *Phil. Mag.* **16** (1967) 749.
12. A. KRELL, *Kristall und Technik* **15** (1980) 1467.
13. A. G. EVANS and E. A. CHARLES, *J. Amer. Ceram. Soc.* **59** (1976) 371.
14. K. H. LEE and J. H. CRAWFORD, Jr, *Appl. Phys. Lett.* **33** (1978) 273.
15. Ji. KVAPIL, Z. VITAMVAS, B. PERNER, Jos. KVAPIL, B. MANEK, O. ADAMETZ and J. KUBELKA, *Kristall und Technik* **15** (1980) 859.
16. R. MELTON, N. DANIELY and T. J. TURNER, *Phys. Stat. Sol. (a)* **57** (1980) 755.
17. A. KRELL, thesis, AdW der DDR, 1981.
18. F. FRÖHLICH, P. GRAU and W. GRELLMANN, *Phys. Stat. Sol. (a)* **49** (1977) 79.
19. W. POMPE, H.-A. BAHR, G. GILLE and W. KREHER, *J. Mater. Sci.* **13** (1978) 2720.
20. W. KREHER and W. POMPE, *J. Mater. Sci.* **16** (1981) 694.
21. W. POMPE, A. KRELL and W. KREHER, unpublished work.
22. F. F. LANGE, *Phil. Mag.* **22** (1970) 983.
23. A. G. EVANS, *ibid.* **26** (1972) 1327.
24. A. I. A. ABDEL-LATIF, R. E. TRESSLER and R. C. BRADT, in "Fracture '77" Vol. 3 edited by D. M. R. Taplin (University of Waterloo Press, Waterloo, Ontario, 1977) p. 933.
25. H. ENDL and H. HAUSNER, *Ber. Dt. Keram. Ges.* **57** (1980) 128.
26. R. A. EVARESTOV, A. N. ERMOSHKIN and V. A. KOVCHIKOV, *Phys. Stat. Sol. (b)* **99** (1980) 387.
27. H. ENDL and H. HAUSNER, *Ber. Dt. Keram. Ges.* **57** (1980) 121.
28. B. N. DAS, *J. Mater. Sci.* **10** (1975) 1246.
29. G. DUFEK, A. VENDL, W. WRUSS and R. KIEFFER, *Ber. Dt. Keram. Ges.* **53** (1976) 336.

Received 27 July
and accepted 4 November 1981